



**HAL**  
open science

## Influence of deposition strategy on porosity in powder-feed directed energy deposition (DED)

Neha Devi Dhoonooah, Kamel Moussaoui, Frederic Monies, Walter Rubio,  
Redouane Zitoune

► **To cite this version:**

Neha Devi Dhoonooah, Kamel Moussaoui, Frederic Monies, Walter Rubio, Redouane Zitoune. Influence of deposition strategy on porosity in powder-feed directed energy deposition (DED). 27th International ESAFORM Conference on Material Forming, Apr 2024, Toulouse, France. pp.325-333, 10.21741/9781644903131-37 . hal-04844000

**HAL Id: hal-04844000**

**<https://hal.science/hal-04844000v1>**

Submitted on 17 Dec 2024

**HAL** is a multi-disciplinary open access archive for the deposit and dissemination of scientific research documents, whether they are published or not. The documents may come from teaching and research institutions in France or abroad, or from public or private research centers.

L'archive ouverte pluridisciplinaire **HAL**, est destinée au dépôt et à la diffusion de documents scientifiques de niveau recherche, publiés ou non, émanant des établissements d'enseignement et de recherche français ou étrangers, des laboratoires publics ou privés.

## Influence of deposition strategy on porosity in powder-feed directed energy deposition (DED)

DHOONOOAH Neha Devi<sup>1,a\*</sup>, MOUSSAOUI Kamel<sup>1,b</sup>, MONIES Frederic<sup>1,c</sup>, RUBIO Walter<sup>1,d</sup>, ZITOUNE Redouane<sup>1,e</sup>

<sup>1</sup>Institut Clément Ader (ICA), UMR-CNRS 5312, "INSA, UPS, Mines Albi, ISAE", Université de Toulouse, 133 C Avenue de Rangueil, 31077 Toulouse, France

<sup>a</sup>neha-devi.dhoonooah@univ-tlse3.fr, <sup>b</sup>Kamel.MOUSSAOUI@isae-superaero.fr, <sup>c</sup>frederic.monies@univ-tlse3.fr, <sup>d</sup>walter.rubio@univ-tlse3.fr, <sup>e</sup>redouane.zitoune@jut-tlse3.fr

**Keywords:** DED-Powder, Deposition Strategy, Automatic Toolpath Generation, Surface Roughness, Bearing Ratio Curve

**Abstract.** Directed energy deposition (DED) is an additive manufacturing process which is increasingly being used for direct manufacturing, added function application and component repair of high-value metals and alloys that are otherwise hard to machine conventionally [1]. However, most commercially available toolpath generators are not comprehensive with regards to the deposition strategy and process parameters, emphasis usually being placed solely on the overlap of adjacent weld beads rather than including the interaction between the contour curves and infill pattern. This increases the probability of gap formation in the deposition pattern, and hence the rate of porosity in the part. This study focuses on the influence of varying bead overlap on the resulting bead geometry and surface roughness for Inconel 718 workpieces deposited using the DED process. The deposition strategy was devised using Python programming language, and the code found to be robust for both single- and multi-layer deposits.

### Introduction

The laser DED process uses a focused source of thermal energy to fuse material, generally in powder or wire form, for building 3D shapes through layer-by-layer deposition. Widely used in the aerospace, military and medical sectors, DED may be used for depositing titanium-, nickel- and iron-based alloys, as well as different grades of stainless steel, with a relatively higher deposition rate than other common AM processes [2]. Moreover, it usually results in a smaller heat affected zone (HAZ) than other welding-based repair methods such as submerged arc welding [2]. The DED process depends on the interaction of several process parameters such as laser power, scanning speed and material feed rate. Another parameter which remains crucial for the process optimisation is the deposition strategy. In fact, several authors have shown that this parameter is the key to obtaining a good visual and structural finish, as well as minimising the occurrence of porosities and voids in the printed part.

It is important to note that porosities are defects that commonly occur in metal AM parts, negatively affecting their mechanical properties. The origin of the porosity may come from the powder feedstock or the process itself [3]. Powder-induced pores result from the entrapment of the carrier gas inside the feedstock during powder atomisation and are generally spherical in shape. These can directly affect as-fabricated parts and degrade their overall performance. Process-induced pores occur when the applied thermal energy is insufficient for complete melting of the feedstock, or when spatter of the powdered material occurs. These pores are typically non-spherical in shape and occur in a variety of sizes, ranging from the sub-microscopic to the macroscopic size. As highlighted by Sames et al. [4], porosity is directly influenced by process methodology, and so process parameters need to be accurately tuned to minimise the risk of pore

formation. The occurrence of porosity or voids at the part surface or within the part effectively reduce density.

In a single printed layer, the overlap between adjacent weld beads needs to be monitored to prevent voids, and hence improve the density of the part. As layers are stacked, new process requirements arise due to the complex thermal activity occurring between consecutive layers. When the laser source moves over a previously deposited layer, thermal energy accumulates and this causes a partial re-melting of this particular layer, hence affecting the HAZ, formed microstructure and overall part density. The selected deposition strategy for a particular process has a significant influence on the density and microstructure of the resulting part.

This study looks at the influence of varying bead overlap on the resulting bead geometry and surface roughness for Inconel 718 workpieces deposited using the DED process. While the influence of adjacent bead overlap has already been studied extensively for the laser powder bed fusion (LPBF) process, our approach of using bearing ratios for characterising deposits achieved using varying bead overlaps in powder-feed laser metal deposition (LMD) is novel and could potentially prove to be significant. A toolpath generation approach for metal powder DED was developed using Python programming language and tested through the physical printing of individual weld beads, and single- and multi-layered geometries with Inconel 718 powder on a BeAM® laser deposition machine. The bead geometry, extent of porosity in the prints, and surface roughness were then evaluated using an Alicona® microscope.

### **Selection of the deposition strategy**

The majority of deposition strategies currently used in AM processes are based on those used in computer-aided machining (CAM) software, such as for milling operations. While the principles behind the strategies used for subtractive and additive processes remain the same, it is important to note that AM includes aspects such as adjacent weld bead overlap, laser spot size, weld bead cross-sectional diameter, etc., which determine the overall thermal activity occurring during a 3D build. These need to be optimised in order to produce parts with a good microstructure, minimum porosity and high density, as well as better mechanical properties, minimal distortion and thermal stresses.

Deposition strategies were experimentally assessed by Parimi et al. [6] to optimise the microstructure of Inconel 718 deposited through the DED process. They used unidirectional and bidirectional deposition paths, as well as different laser power values ranging from 390 to 910W but did not conclude on a preference for either deposition strategy. Ribeiro et al. [2] studied the influence of weld bead stepover on the production of stainless steel 316 cubes using the DED process and concluded that the contour toolpath resulted in the best performance, closely followed by the zigzag. Both these strategies were linked to more uniform heat distribution and less distortions for similar deposition heights. Calleja et al. [7] tested new process parameters and strategies for optimising multi-axis laser cladding operations with AISI 1045 structural steel as substrate material and an AISI 316L stainless steel as filler material. For cladding a hemispherical surface, they concluded that a hatching strategy comprising horizontal, vertical and 45°-diagonal strategies resulted in the best-quality deposition, the combination of angles creating a “mesh type” structure, with optimal overlapping and a uniform 3D structure [7].

In this study, we initially considered combinations of different modes (one-way, zigzag and oscillatory) and directions (horizontal, vertical, and 45°-diagonal) for the generation of automatic toolpaths, where the toolpath here refers to the set of movements of the deposition head during the layer-by-layer deposition process. The zigzag mode has been found to be the most commonly used in material deposition due to its ease of implementation and independence of the shape of the cross-section. It can therefore be used for depositing various thin or thick shapes [2]. In view of the oblong-shaped single- and multi-layer geometries that we intend to study, we thus selected the horizontal zigzag strategy for its relatively long strokes between the start and end points of the

toolpath. As compared to the vertical zigzag, this is expected to result in lower heating, fewer burn marks, and fewer voids at the edges of the infill pattern.

## Methodology

### *Deposition of single-layer geometries*

In order to evaluate the influence of deposition strategy and bead overlap on the final geometry of DED deposited parts, Inconel 718 workpieces in the shape of oblongs with length 20mm and width 10mm were deposited onto a 4mm-thick substrate of the same material, using a BeAM® machine. Based on previous tests, the laser power (P) was set to 250W, with scanning speed (v) of 1300mm/min and powder feed rate of 6.50g/min – all parameters remaining constant throughout the process. With these parameters, the average bead width and height resulted in 0.56mm and 0.2mm respectively.

Prior to the deposition process, a control set of three individual weld beads were deposited at the edge of the substrate to set a reference value of bead height for the selected values of P and v. This was repeated at the end of the deposition process to compare the measurements and hence assess the reproducibility of the process. Using an Alicona® microscope, the average bead height was found to be 0.25mm prior to deposition and 0.26mm post-deposition, indicating good repeatability over the duration of the process.

The overlap between adjacent weld beads,  $R_{cent}$ , was set to 10%, 30% and 50% to determine the effective average height of the deposited pattern, the deposition quality, and the roughness characteristics. For each value of  $R_{cent}$ , the oblong pattern was deposited three times to ensure the repeatability and reproducibility of the process.

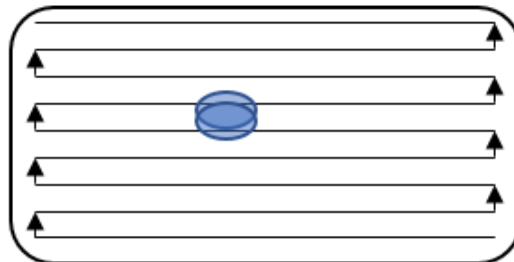


*Fig.1: A diagram illustrating the overlap between adjacent beads in the deposit zone*

### *Deposition of multi-layer geometries*

The same values of laser power, scanning speed and powder feed rate were further used to deposit 10-layer-high stacks, with a constant Z-increment of 0.2mm, and overall nominal height of 2.0mm. According to Ribeiro et al. [2], this Z-increment likely needs to be adjusted to compensate for decreases in layer thickness as layers are stacked to build higher workpieces. However, this was not considered in this study so that any reduction in the resulting average height of the stacks could be detected.

During deposition in Z, the focal distance for both the powder feedstock and laser source was set to 3.5mm. It was verified that small variations around the focal point of the laser did not significantly influence the laser spot size and geometry of the weld beads, even when varying the values of bead overlap.

## Results and discussion

The single- and multi-layer geometries were both analysed for dimensional accuracy in terms of bead width and height, and quality of deposition according to roughness characteristics.

Similarly to the measurement process for the individual beads, the average height of each layer was measured at three points along each of three sections under the Alicona® microscope. Measurements were taken at the highest point of the profile of a given section. They were averaged first across the section, then across the given deposit. To characterise the roughness of the

deposited surface, the average roughness of the profile through a given cross-section,  $R_a$ , and the maximum peak-to-valley height of the same given profile,  $R_t$ , were also measured using the microscope.

As in Fig.2 below, no open and/or closed pores were visibly present in the deposits, indicating that the deposition process did not generate important defects in the printed parts. The increasing bead overlap resulted in adjacent weld beads lying closer to each other. For lower overlap values, a larger and shallower melt pool forms across adjacent beads, resulting in a lower degree of fusion across the material deposits, and hence higher effective heights. As the bead overlap increases, the distance between the centres of adjacent bead decreases and this results in the formation of deeper melt pools. Further, more thermal energy is imparted to the substrate and feedstock during the partial re-melting that occurs as the laser source moves in a zigzag pattern. More feedstock gets fused in these deeper melt pools, and hence less of it is present above substrate level.



*Fig. 2: A visual representation of how the deposition pattern evolves with varying bead overlap, from 10% to 30% to 50%*

For the single-layer deposits, bead height was seen to decrease significantly as  $R_{cent}$  increases from 10% to 50%, as summarised in Table 1 below. The nominal height of 0.25mm for the single weld beads deposited at the start of the study reduced by 20% for the 10%-overlap single-layer geometry, while it dropped by around 50% for the 50%-overlap geometry, indicating a significant change in the definition of the melt pool and amount of feedstock fused to the substrate.

*Table 1: Average dimensions of weld bead height for both single- and multi-layer geometries*

Bead overlap (%)	Average bead height/mm		Deviation from nominal height (%)	
	For single-layer deposits	For 10-layer 3D stacks	For single-layer deposits	For 10-layer 3D stacks
10	0.20	0.16	20	36
30	0.14	0.14	44	44
50	0.13	0.11	48	56

For the multi-layer geometries, the average bead height decreased similarly with an increase in overlap, but this decrease was more significant than for the single-layer deposits. As layers are stacked in the DED process, the zigzag movement of the laser beam above the previously deposited layer gives rise to partial re-melting of this layer, creating a deeper melt pool and further absorption of the metallic powder into the said layer. This causes stacked layers to fuse to a greater extent

with one another as the laser moves in the positive Z-direction, and results in a much lower average bead height than expected, as compared to the nominal value of 0.25mm.

Increasing bead overlap also leads to the formation of deeper melt pools and both these factors combine to create a more significant decrease in average bead height for the multi-layered geometries than for the single layers, as seen from the values in Table 1. In the case of 30% bead overlap however, no difference was observed in the height deviation between single- and multi-layered geometries, which seems to indicate a good and uniform extent of dilution between the surface of the substrate and the first deposited layer, as well as between the stacked layers themselves. Both the single- and multi-layered samples deposited with a 30% bead overlap have been retained for further analysis of the microstructure to confirm these findings.

A similar decreasing trend was seen in the average values of  $R_a$  and  $R_t$  for increasing bead overlap in both single- and multi-layer geometries, as summarised in Table 2 below, indicating a smoother and more uniform surface finish with lower peak-to-valley heights across a given profile. For lower overlap values, the melt pool forms predominantly on the previously deposited weld bead and less so on the adjacent one. As the bead overlap increases, the melt pool forms over a larger surface area, the powdered feedstock gets fused more uniformly, and this results in a lower, smoother geometry with markedly lower roughness.

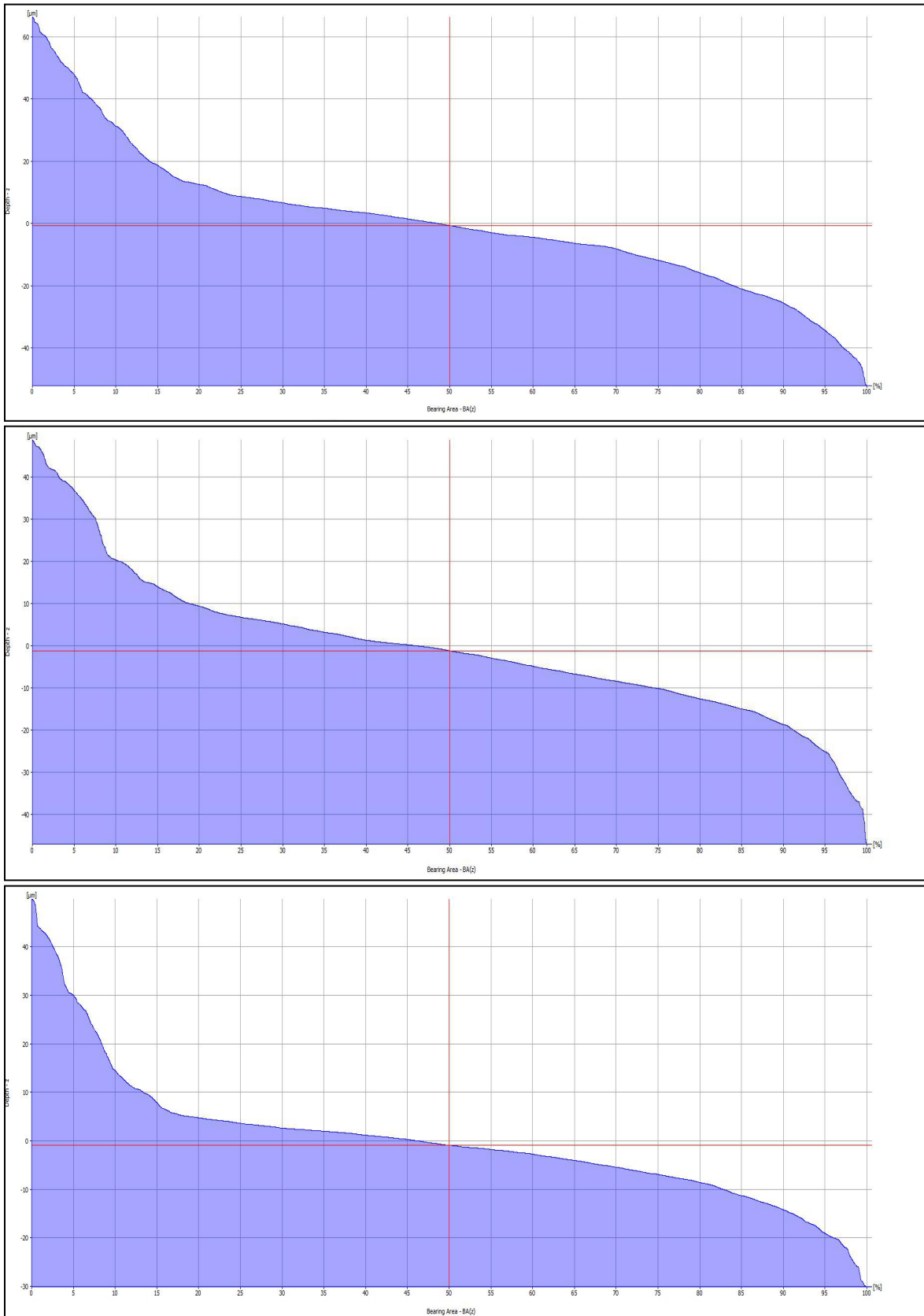
*Table 2: Average dimensions of  $R_a$  and  $R_t$  for both single- and multi-layer geometries*

Bead overlap (%)	Average $R_a/\mu\text{m}$		Average $R_t/\mu\text{m}$	
	For single-layer deposits	For 10-layer deposits	For single-layer deposits	For 10-layer deposits
10	17.17	14.58	122.52	114.21
30	13.92	10.31	99.24	91.85
50	10.95	7.73	87.78	77.17

In order to qualify the rate of material deposition, the roughness profiles and bearing ratio curves were analysed for the different bead overlaps in both single- and multi-layer deposits. The bearing ratio curve, also known as the Abbott-Firestone curve is a qualitative measure of the surface texture of an object, where the curve is calculated from a roughness profile by drawing lines parallel to the datum and measuring the extent of the line that lies within the profile [8].

As seen in Figs. 3-5 below, the rate of material deposition for the single-layer geometries decreased faster with increasing bead overlap, with a noticeably sharper decrease from 30 to 50%, as compared to 10 to 30%. The average profile roughness was seen to reduce by over 35% while the average peak-to-valley height values dropped by almost 30%.

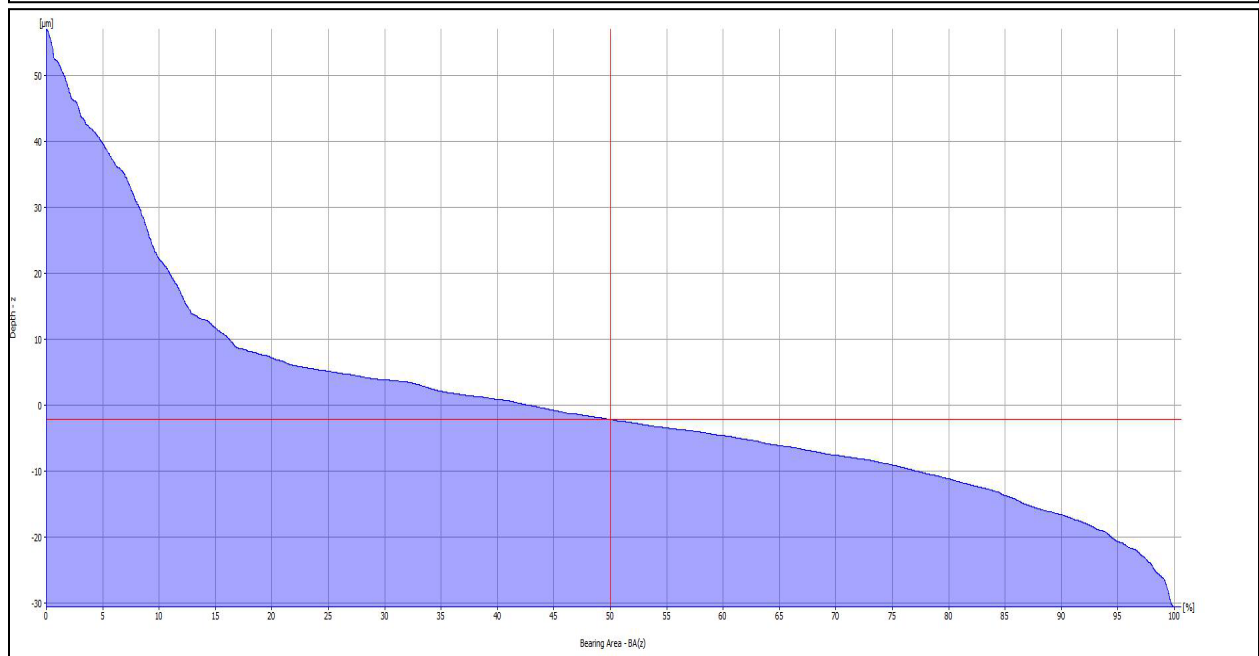
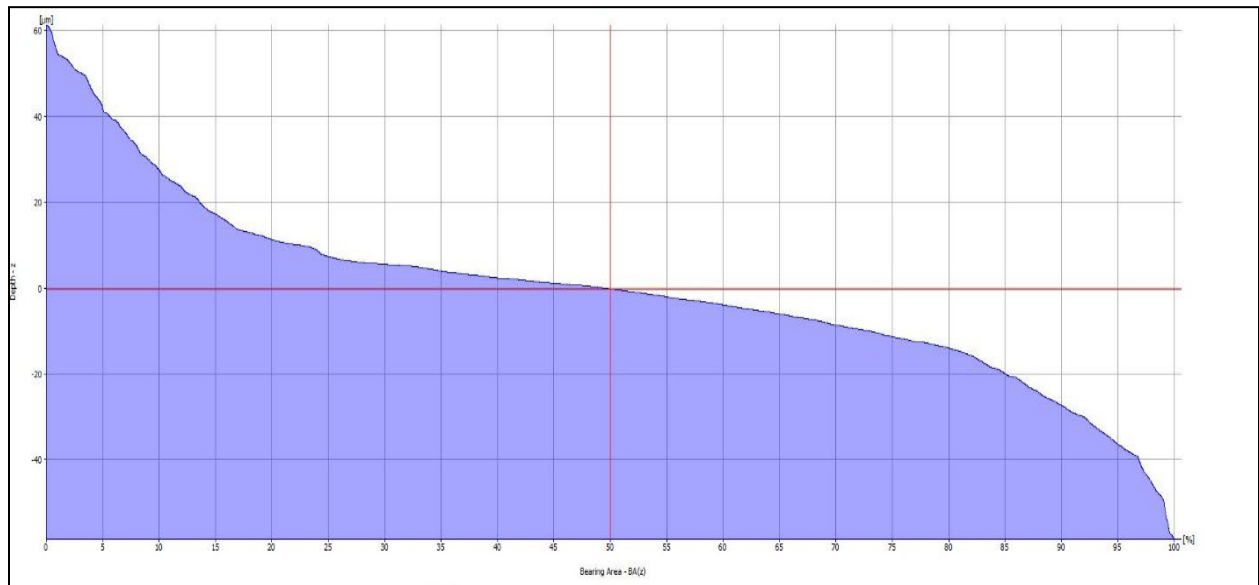
As bead overlap increases, adjacent weld beads lie closer to each other, and the melt pools formed are also deeper as described previously. More feedstock gets fused at the surface of the substrate, so that the average peak-to-valley height reduces, and more material is contained below the material line drawn to estimate the bearing ratio. The steeper gradient above the 50%-mark in the bearing ratio curve for the 50% bead overlap indicates a fewer number of peaks in a deposition pattern that is highly uniform and mostly planar due to the adjacent beads lying closer. Less material is contained in the series of peaks lying above the average material surface, and hence a sharp decline in the rate of material deposition is seen.



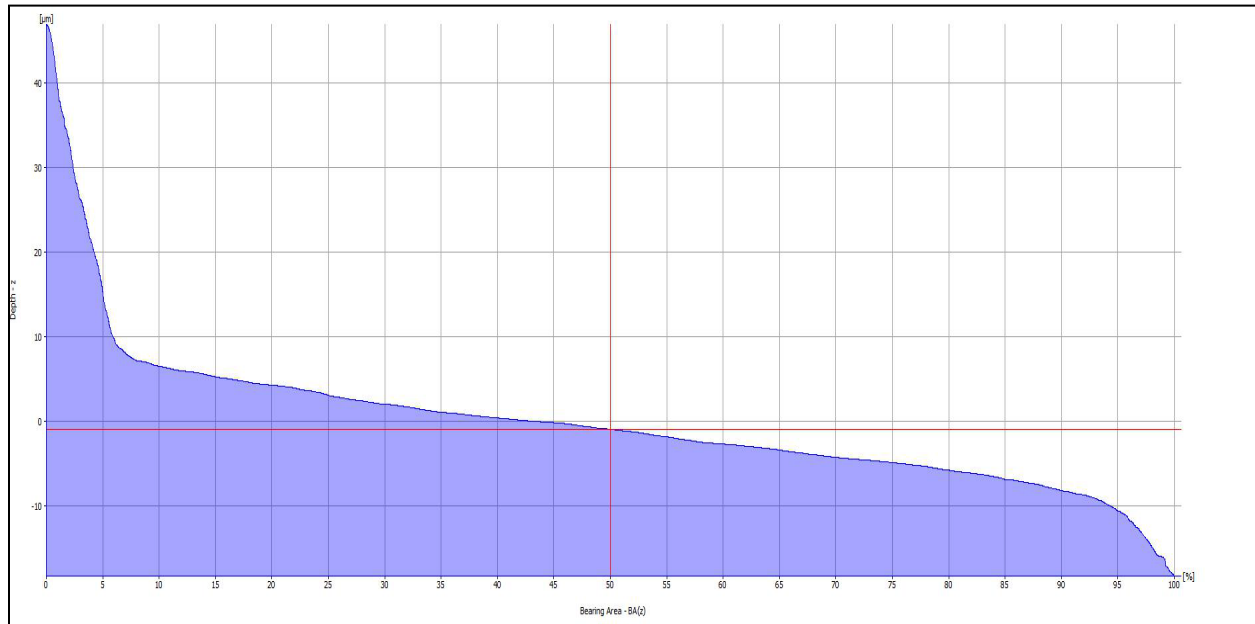
*Figs.3-5: Bearing ratio curves for single-layer deposits, showing steeper declines in the rate of material deposition with increasing bead overlap (top to bottom)*

As bead overlap increased from 10 to 50% in the multi-layer deposits, the average profile roughness was seen to reduce by over 45% while the average peak-to-valley height values dropped by over 30%. This trend was similar to that observed for the single-layer deposits where the melt pool is both deeper and more uniform across closer adjacent weld beads.

A more pronounced drop in the rate of material deposition was observed as in Figs. 6-8 below. This is due to the additional movement of the laser beam in Z as it fuses successive layers, causing repeated melting and solidification cycles as the stack rises. This leads to partial re-melting between the stacked layers, forming deeper melt pools and resulting in even lower average peak-to-valley heights across the top surface of multi-layered deposits as compared to single-layer surfaces. The average value of profile roughness for a stack with 10% bead overlap was 15% lower than that for a single layer, and this rose to almost 30% for the 50% bead overlap.







*Figs.6-8: Bearing ratio curves for multi-layer deposits, illustrating steeper declines than for single-layers as the bead overlap increases (top to bottom)*

### Conclusions and perspectives for further work

From the set of experiments performed in this study on the influence of deposition strategy on bead geometry and surface roughness in powder-feed DED, the following conclusions can be drawn:

- better control of the toolpath generator makes it more robust and suitable for obtaining the desired bead geometry and reducing surface roughness,
- the horizontal zigzag deposition strategy was suitable for depositing geometrically accurate and high-quality single- and multi-layer geometries,
- increasing bead overlap from 10 to 50% resulted in lower average bead height for both the single- and multi-layer geometries, in direct correlation with the formation of deeper, narrower melt pools across adjacent weld beads,
- the 30% bead overlap seems optimal for the DED deposition process since it results in the same average bead height for both single- and multi-layered geometries, indicating a uniform extent of dilution,
- an increase in bead overlap also reduced the roughness characteristics for both types of deposit in line with the changed melt pool definition. Material deposition decreased at a faster rate as shown by the bearing ratio curves, indicating a higher proportion of fused feedstock below the average deposition line, and hence a better, smoother surface finish.

In view of these results, further analysis will be carried out on the deposited samples to characterise the resulting extent of porosity. For the multi-layer deposits, cuts will be made in the samples to observe the cross-section and measure the porosity within and between the successive layers, as a means of characterising the influence of the deposition strategy on defects occurring in the printed parts. The extent of dilution resulting from the varying bead overlap will also be studied to confirm the suitability of using 30% bead overlap for further material deposition.

Moreover, most commercially available toolpath generators are not comprehensive with regards to the deposition strategy and process parameters, emphasis usually being placed only on adjacent weld bead overlap rather than including the interaction between the contour curves and

infill pattern. This increases the probability of gap formation in the deposition pattern, and hence the rate of porosity in the part. When building multi-layer geometries, porosity-related defects will accumulate and eventually lead to irreparable construction defects and a drop in density, as well as mechanical properties [2,5].

In future studies, we propose to investigate the influence of contours delimiting the deposition region, as well as the overlap between the end portion of the weld beads and this contour, and the overlap between the contour and first deposited bead. By definition, these overlaps are not independent of the bead overlap, and the interaction between them is expected to be significant with respect to the resulting bead geometry, surface finish, and extent of porosity.

## References

- [1] Optomec, 2019. How 3D Metal Printing Saves Time and Lowers Costs: DED for Repair of Industrial Components [pdf] <https://optomec.com/wp-content/uploads/2019/03/DEDWebinar-slides.pdf>
- [2] Ribeiro, K.S.B., Mariani, F.E., Coelho, R.T., 2020. A Study of Different Deposition Strategies in Direct Energy Deposition (DED) Processes. *Procedia Manufacturing* 48, 663–670. <https://doi.org/10.1016/j.promfg.2020.05.158>
- [3] Sames, W. J., Medina, F., Peter, W. H., Babu, S. S., Dehoff, R. R., 2014. Effect of Process Control and Powder Quality on Inconel 718 Produced Using Electron Beam Melting. in *Superalloy 718 and Derivatives*, Pittsburgh, PA.
- [4] Sames, W.J., List, F.A., Pannala, S., Dehoff, R.R., Babu, S.S., 2016. The metallurgy and processing science of metal additive manufacturing. *International Materials Reviews* 61, 315–360. <https://doi.org/10.1080/09506608.2015.1116649>
- [5] Flores, J., Garmendia, I., Pujana, J., 2019. Toolpath generation for the manufacture of metallic components by means of the laser metal deposition technique. *Int J Adv Manuf Technol* 101, 2111–2120. <https://doi.org/10.1007/s00170-018-3124-1>
- [6] Parimi, L., L., Ravi, G. A., Clark, D., Attallah, M.M., 2014. Microstructural and texture development in direct laser fabricated IN718. *Materials Characterization* 89:102-111
- [7] Calleja, A., Tabernero, I., Fernández, A., Celaya, A., Lamikiz, A., López de Lacalle, L.N., 2014. Improvement of strategies and parameters for multi-axis laser cladding operations, *Optics and Lasers in Engineering*, Vol. 56, pp. 113-120, ISSN 0143-8166, <https://doi.org/10.1016/j.optlaseng.2013.12.017>
- [8] Johnson, K. L., 1985. *Contact Mechanics*. Cambridge: Cambridge University Press. <https://doi.org/10.1017/CBO9781139171731>